Journal of Microbiology (2019) Vol. 57, No. 10, pp. 910–917
DOI 10.1007/s12275-019-9354-6
eISSN 1976-3794
pISSN 1225-8873

RNase G controls *tpiA* mRNA abundance in response to oxygen availability in *Escherichia coli*

Jaejin Lee[†], Dong-Ho Lee[†], Che Ok Jeon[*], and Kangseok Lee[*]

Department of Life Science, Chung-Ang University, Seoul 06974, Republic of Korea

(Received Jul 16, 2019 / Revised Jul 19, 2019 / Accepted Jul 19, 2019)

Studies have shown that many enzymes involved in glycolysis are upregulated in *Escherichia coli* endoribonuclease G (*rng*) null mutants. However, the molecular mechanisms underlying the RNase G-associated regulation of glycolysis have not been characterized. Here, we show that RNase G cleaves the 5′ untranslated region of triosephosphate isomerase A (*tpiA*) mRNA, leading to destabilization of the mRNA in *E. coli*. Nucleotide substitutions within the RNase G cleavage site in the genome resulted in altered *tpiA* mRNA stability, indicating that RNase G activity influences *tpiA* mRNA abundance. In addition, we observed that *tpiA* expression was enhanced, whereas that of RNase G was decreased, in *E. coli* cells grown anaerobically. Our findings suggest that RNase G negatively regulates *tpiA* mRNA abundance in response to oxygen availability in *E. coli*.

Keywords: glycolysis, mRNA abundance, *rng*, RNase G, *tpiA*

Introduction

Modulation of mRNA stability allows bacterial cells to rapidly adapt to environmental changes. In bacteria, mRNA stability is mainly regulated by several types of ribonucleases (RNases) with diverse sequence specificities (Hui *et al.*, 2014; Mohanty and Kushner, 2016). In *Escherichia coli*, internal cleavage by endoribonucleases such as RNase E, RNase G, RNase III, and RNase P is critical for mRNA processing and degradation (Jain, 2002; Kushner, 2004; Deutscher, 2006; Sim *et al.*, 2010; Lim *et al.*, 2015). Among these endoribonucleases, RNase G, encoded by the *rng* gene, has been identified as an enzyme that generates the mature 5′ end of 16S rRNA (Li *et al.*, 1999; Wachi *et al.*, 1999). RNase G presents high similarity with the N-terminal catalytic region of RNase E (Wachi *et al.*, 1997, 1999), a ribonuclease known to control the stability of thousands of mRNA species (Bernstein *et al.*, 2002; Lee *et al.*, 2002, 2003). Both RNase G and RNase E cleave AU-rich, single-stranded RNA regions in a 5′ end-dependent manner (Tock *et al.*, 2000). Despite the similarities between these enzymes, deletion of the *rng* gene only affects the abundance of a few mRNAs (Lee *et al.*, 2003), indicating that they have distinct physiological roles. For example, incomplete processing of the 5′ terminus of 16S rRNA by downregulation of RNase G can induce resistance to aminoglycoside antibiotics in *E. coli* (Song *et al.*, 2014).

Genome-wide analyses of mRNA abundance indicated that RNase G expression levels are associated with the abundance of mRNA species of genes encoding enzymes involved in carbohydrate metabolism, including *acs*, *adhE*, *eno*, *glk*, *nagB*, *pgi*, and *tpiA* (Lee *et al.*, 2002). For the *eno* gene, a simultaneous increase in mRNA abundance and protein levels has been observed in *rng*-deleted cells (Kaga *et al.*, 2002). However, the molecular mechanisms underlying RNase G-associated regulation of the expression of these genes have not been characterized. Therefore, in this study, we examined the functional role of RNase G in expression of the *tpiA* gene that also codes for a glycolytic enzyme, the mRNA abundance of which is increased by deletion of the *rng* gene. Additionally, we also investigated the physiological relevance of RNase G in modulating the abundance of mRNA species encoding enzymes involved in carbohydrate metabolism.

Materials and Methods

Bacterial strains and plasmid construction

The strains, plasmids, and primers used in this study are listed in Tables 1 and 2. *E. coli* strains were grown at 37°C in Luria-Bertani (LB) medium under aerobic or anaerobic conditions. For anaerobic growth of *E. coli* cells, a 30 ml cylindrical bottle containing a sterilized stir bar was filled with LB media fully and sealed with a sealing tape then cultured on the magnetic stirrer. The MG1655*rng* strain has been previously described (Song *et al.*, 2014). The tpiA-5′-UTR-MT plasmid was constructed using the CRISPR-Cas9 system as described below and the pCas and pTargetF plasmids were used (Addgene plasmid # 62225 and 62226; Addgene). pTargetT-na(N_{20}) and pTargetT-ar(N_{20}) were constructed by insertion of homologous DNA into pTargetF-na(N_{20}) and pTargetF-ar(N_{20}). To clone the *tpiA* target N_{20} sequence into pTargetF, a DNA fragment containing a 20 bp native protospacer (N_{20}) of the 5′ UTR of the *tpiA* gene was amplified using the Np1/Np2 primers, digested with *Spe*I and *Eco*RI, and then ligated into pTargetF. To construct pTargetT-na(N_{20}), 600 bp of homologous DNA containing a 20 bp artificial protospacer was amplified by overlap-extension PCR

[†]These authors contributed equally to this work.
*For correspondence. (K. Lee) E-mail: kangseok@cau.ac.kr; Tel.: +82-2-820-5241; Fax: +82-2-825-5206 / (C.O. Jeon) E-mail: cojeon@cau.ac.kr; Tel.:+82-2-820-5864; Fax: +82-2-825-5206

Table 1. Strains and plasmids used in this study

Strains	Relevant characteristics	Reference
E. coli MG1655	F^- lambda$^-$ *ilvG-rfb-50 rph-1*	Laboratory strain
E. coli MG1655*rng*	MG1655 but with Δ*rng*	Lee *et al.* (2002)
tpiA-5′-UTR-MT	MG1655 but with nucleotide substitutions at −33 and −34 of the 5′ UTR of *tpiA* mRNA	In this study
Plasmids		
pTargetF	*pMB1 aadA* sgRNA-*cadA*	Addgene: 62226
pTargetF-na(N_{20})	*pMB1 aadA* sgRNA-*tpiA*(N_{20})	This study
pTargetF-ar(N_{20})	*pMB1 aadA* sgRNA-*artificial*(N_{20})	This study
pTargetT-na(N_{20})	pTargetF-na(N_{20}) but with an artificial N_{20} in the homologous DNA	This study
pTargetT-ar(N_{20})	pTargetF-na(N_{20}) but with UU substituted for GG at −33 and −34 in the 5′ UTR of the homologous DNA	This study
pCas	*repA101*(Ts) Km^R P_{cas}-*cas9* P_{araB}-*Red lacI*^{q} P_{trc}-sgRNA-*pMB1*	Addgene: 62225
pKAN6B	*p15A ori,* Km^R	Yeom *et al.* (2008)
pKAN6-RraA	*p15A ori,* Km^R, *rraA* under P_{araB}	Yeom and Lee (2006)

using the Hp1/Hp2 and Hp3/Hp4 primers. Two PCR products were combined and amplified using the Hp1/Hp4 outside primers, digested with *Eco*RI and *Hin*dIII, and then cloned into pTargetF-na(N_{20}). Similarly, pTargetT-ar(N_{20}) was also constructed by inserting a 20 bp artificial protospacer (N_{20}) and homologous DNA containing the substituted nucleotides. To insert the artificial target N_{20} sequence into pTargetF, the PCR product amplified using the Ap1 and Ap2 primers, containing a 20-bp artificial N_{20}, was cloned into pTargetF after enzyme digestion with *Spe*I and *Eco*RI. To construct pTargetT-ar(N_{20}), the PCR product obtained with the Hp1/Hp5 and Hp4/Hp6 primers was cloned into pTargetF-ar(N_{20}), as described above.

Western blot analysis

Western blot analysis was carried out as described in a previous study (Song *et al.*, 2017). Briefly, proteins were resolved on 10% sodium dodecyl sulfate (SDS) polyacrylamide gels, and the gels were electroblotted onto a nitrocellulose membrane. Images of the western blots were obtained using a ChemiDoc™ Imaging System (Bio-Rad Laboratories) and quantified using Quantity One (Bio-Rad Laboratories). The ribosomal protein S1 was used as the internal control.

RNA preparation and quantitative real time-polymerase chain reaction (RT-PCR)

Total cellular RNA was extracted from cultures grown to mid-log phase using the RNeasy mini prep kit (Qiagen). For measurement of the *tpiA* mRNA half-life, bacterial cell cultures were harvested at 1, 2, 4, and 8 min after rifampicin addition (1 mg/ml). The RT-PCR analysis was performed as previously described (Baek *et al.*, 2018). Briefly, cDNA was synthesized from 0.5 μg of total RNA using a PrimeScript™ 1st strand cDNA Synthesis Kit (TaKaRa). Samples were prepared to a final volume of 10 μl using iQ™ SYBR® Green Supermix (Bio-Rad Laboratories) and real-time RT-PCR was performed on a CFX-96 Thermal Cycler and Detection System (Bio-Rad Laboratories).

Table 2. Primers used in this study

Primers	Sequence (5′→3′)
UTR-F	AGACCTGCTGCCCTGCGG
UTR-R	GGCTGCCGTTCAGTTTCCAG
rnpB-RT-F	TTGCTCCGGGTGGAGTTTAC
rnpB-RT-R	GTGCAACAGAGAGCAAACCG
tpiA+21R	CATCACTAAAGGATGTCGCAT
ladder-tpiA-F	ATAAGAATGCGGCCGCAGACCTGCTGCCCTGCGGGG
ladder-tpiA-R	ATAAGAATGCGGCCGCTTAAGCCTGTTTAGCCGCTTC
Np1	GTCCTAGGTATAATACTAGTCCAGCTCGTGAACCATGTGGGTTTTAGAGCTAGAAATAGC
Np2	CGGAATTCAAAAAAAGCACCGACTCG
Hp1	CGGAATTCTCAGGAATACATGGCAGCGG
Hp2	CAGCTCTCGGCACTGTAATCCGGCTGCCGTTCAGTTTCCA
Hp3	GATTACAGTGCCGAGAGCTGTTTCTAACCTGCGTAAAGAG
Hp4	CCCAAGCTTTACTGTGCGCCGATGTCTT
Hp5	CCACGCTTATAAGCGAATAAAGGBBGATGGCCGCCCCGCAGGGC
Hp6	CCTTTATTCGCTTATAAGCGTGG
Ap1	GGTATAATACTAGTCAGCTCTCGGCACTGTAATCGTTTTAGAGCTAGAAATAGC
Ap2	CGGAATTCAAAAAAAGCACCGACTCG
Cp1	ATGCACAGAACCGGAGTCAG
Cp2	AGAGCAAAAAGCCGCGAAAG

Primer extension analysis

The primer extension analysis was performed as previously described (Song *et al.*, 2019). In brief, 40 μg of total RNA and 5′-^{32}P-labeled primers were hybridized at 65°C for 5 min, and then cooled to 37°C. The extension reaction was performed with AMV reverse transcriptase (New England Biolabs) at 42°C for 1 h, and the extended fragments were analyzed on a 12% polyacrylamide gel containing 8 M urea. The tpiA+21R primer was used for cleavage site analysis of the *tpiA* 5′ UTR. Autoradiography was generated using a Packard Cyclone Phosphor Imager (PerkinElmer) as previously described (Cho *et al.*, 2018).

Purification of RNase G

E. coli RNase G (Rng) was purified from *E. coli* KSL2004 strain using an Ni-NTA agarose and affinity column. The enzyme was eluted from the column using 125 mM imidazole, concentrated, and then stored as previously described (McDowall *et al.*, 1995; Lee *et al.*, 2002; Sun *et al.*, 2018).

In vitro cleavage assay

RNase G cleavage assays were performed as previously described (Lee *et al.*, 2002). In brief, synthetic *tpiA* mRNA containing the 5′ UTR (52 mer, BBI Life Sciences) was labeled at the 5′ end using [γ-^{32}P]ATP and T4 polynucleotide kinase and purified from 12% polyacrylamide gels containing 8 M urea. The 5′-end-labeled *tpiA* transcript (3 pmol) was incubated with purified RNase G (6 pmol) in reaction buffer at 37°C at each time point (1, 10, and 20 min). BSA was used as a negative control.

Nucleotide substitutions using the CRISPR-Cas9 system

The procedure used to substitute the 'UU' for a 'GG' at nucleotide positions -33 and -34 from the transcriptional start site of *tpiA* was performed according to previous studies (Jiang *et al.*, 2015; Wang *et al.*, 2018). Two CRISPR events were performed using pTargeT-na(N_{20}) and pTargeT-ar(N_{20}) with pCas. The MG1655 strain harboring pCas was prepared as previously described (Cha *et al.*, 1997; Sharan *et al.*, 2009). To induce λ-Red recombinase, L-arabinose (10 mM final concentration) was added to an OD_{600} of 0.1. For the first CRISPR event, to avoid a repeated cleavage after homologous recombination, 100 ng of pTargeT-na(N_{20}) was added to 50 μl of electrocompetent cells harboring pCas and transformed by electroporation using a Gene Pulser (2-mm cuvette, Bio-Rad Laboratories) at 2.5 kV. After electroporation, the cells were suspended in 1 ml of LB medium and incubated at 30°C for 1 h. The recovered cells were then spread onto LB agar plates containing spectinomycin (50 mg/ml) and kanamycin (50 mg/ml) and incubated overnight at 30°C. To confirm the transformants, colony PCR and DNA sequencing were performed using the Cp1 and Cp2 primers. pTargetT-na(N_{20}) was cured by incubating in 2 ml of LB medium containing kanamycin (50 mg/ml) and isopropyl β-D-thiogalactoside (1 mM final concentration). Overnight-incubated cultures were spread onto LB plates containing kanamycin (50 mg/ml), and then the sensitivity to spectinomycin was measured to confirm that pTargetT-na(N_{20}) had been cured. To insert the substitute mutant sequence, 100 ng of pTargeT-ar(N_{20}) was added to a temporal mutant harboring pCas. The rest of the procedure was as described above. After successful nucleotide substitution, pTargeT-ar(N_{20}) was cured using

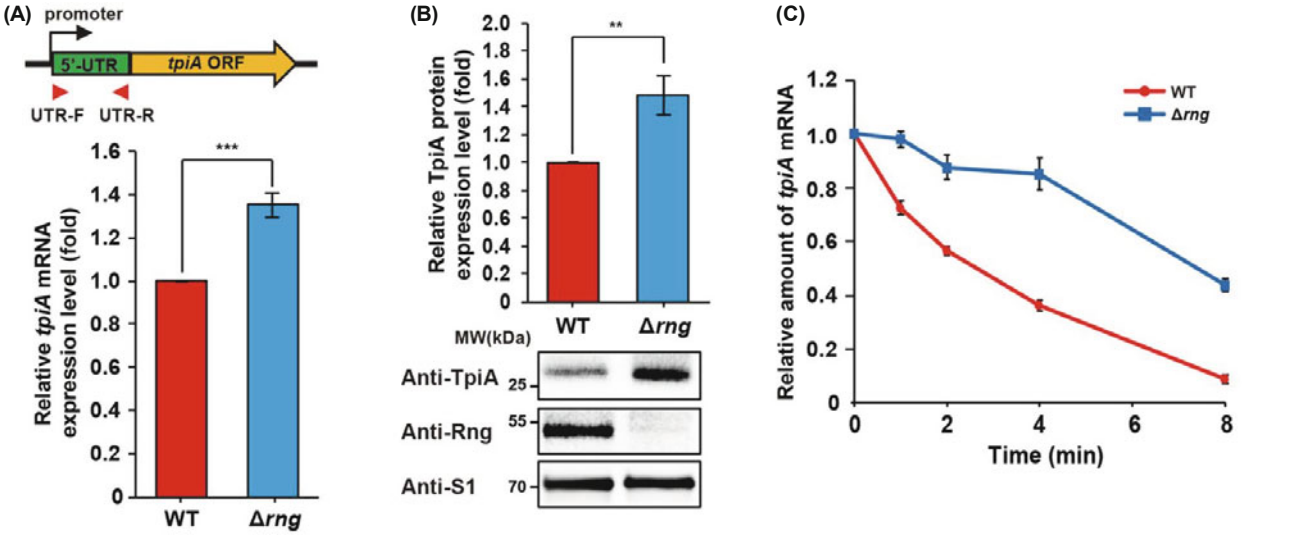

Fig. 1. Effect of RNase G on *tpiA* expression. (A) Analysis of *tpiA* mRNA expression levels. Top: schematic showing the location of the primer binding sites (UTR-F and UTR-R) in the genomic DNA of the *E. coli* MG1655 strain for real-time RT-PCR. Bottom: wild-type (WT) and *rng*-deleted (Δ*rng*) MG1655 cells were cultured at 37°C to an OD_{600} of 0.7, followed by total RNA extraction. cDNA synthesis was performed with 0.5 μg of total RNA using random hexamers, and *tpiA* mRNA expression levels were analyzed by real-time RT-PCR. The expression level of *tpiA* mRNA was normalized to that of *rnpB* mRNA, and gene expression was quantified using the ΔΔCt method. (B) Western blot analysis of TpiA and Rng. *E. coli* cultures used in (A) were collected for western blot analysis of TpiA and Rng using the respective polyclonal antibodies. The TpiA and Rng expression levels were compared by setting those of the WT to 1. The S1 protein was used as an internal standard. (C) Effects of the presence or absence of RNase G on *tpiA* mRNA stability. Total RNA was prepared from *E. coli* cultures used in (A) at 0, 1, 2, 4, and 8 min after the addition of rifampicin (1 mg/ml). cDNA synthesis and quantitation of gene expression were performed as described in the legend to Fig. 1A. For (A), (B), and (C), the data represent the mean ± s. e. m. of three independent experiments. Asterisks indicate significant differences (two-sided, unpaired Student's *t*-test), $^{**}P < 0.005$, $^{***}P < 0.0005$.

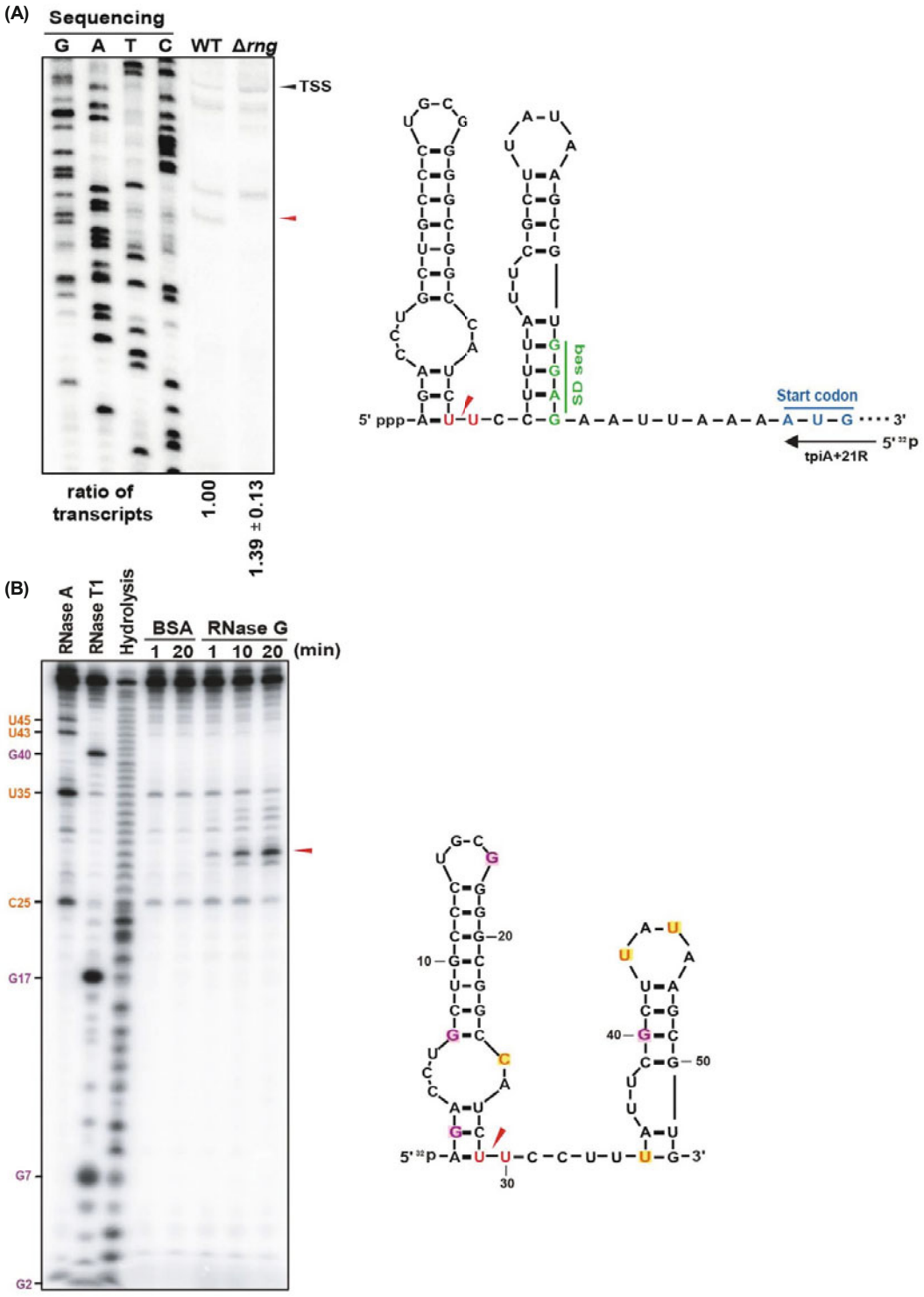

Fig. 2. Identification of RNase G cleavage site in *tpiA* mRNA. (A) Primer extension analysis of the 5′ UTR of *tpiA* mRNA *in vivo*. Left: total RNA was extracted from wild-type (WT) and Δ*rng* MG1655 strains and hybridized with a ^{32}P-5′-end-labeled primer (tpiA+21R). cDNA was synthesized using AMV reverse transcriptase and sequencing ladders were prepared with the same primer used in hybridization; a PCR amplicon containing the 5′ UTR of *tpiA* mRNA was used as a template. Synthesized cDNA products were resolved on a 12% polyacrylamide gel with 8 M urea in TBE. The black and red arrows respectively indicate the transcriptional start site (TSS) of *tpiA* mRNA and the RNase G cleavage product. Right: the secondary structure of the full-length *tpiA* mRNA and that of the 5′ UTR encompassing the RNase G cleavage site (marked in the red) were inferred using M-fold software. The putative Shine-Dalgarno sequence and start codon are indicated in green and blue, respectively. (B) *In vitro* cleavage of *tpiA* synthetic RNA. Left: 3 pmol ^{32}P-5′-end-labeled *tpiA* synthetic RNA oligo (52 mer) was incubated with 6 pmol purified RNase G in cleavage buffer at 37°C. The cleavage samples were collected at the indicated time points and separated as described in (A). Cleavage products were identified using size markers generated by alkaline hydrolysis and RNase T1 and RNase A digestion. Right: predicted secondary structure of the *tpiA* synthetic RNA oligo and RNase G cleavage site (marked in red) were inferred using M-fold software. RNase A cleavage products are indicated in orange bold characters and those of RNase T1 in violet bold characters.

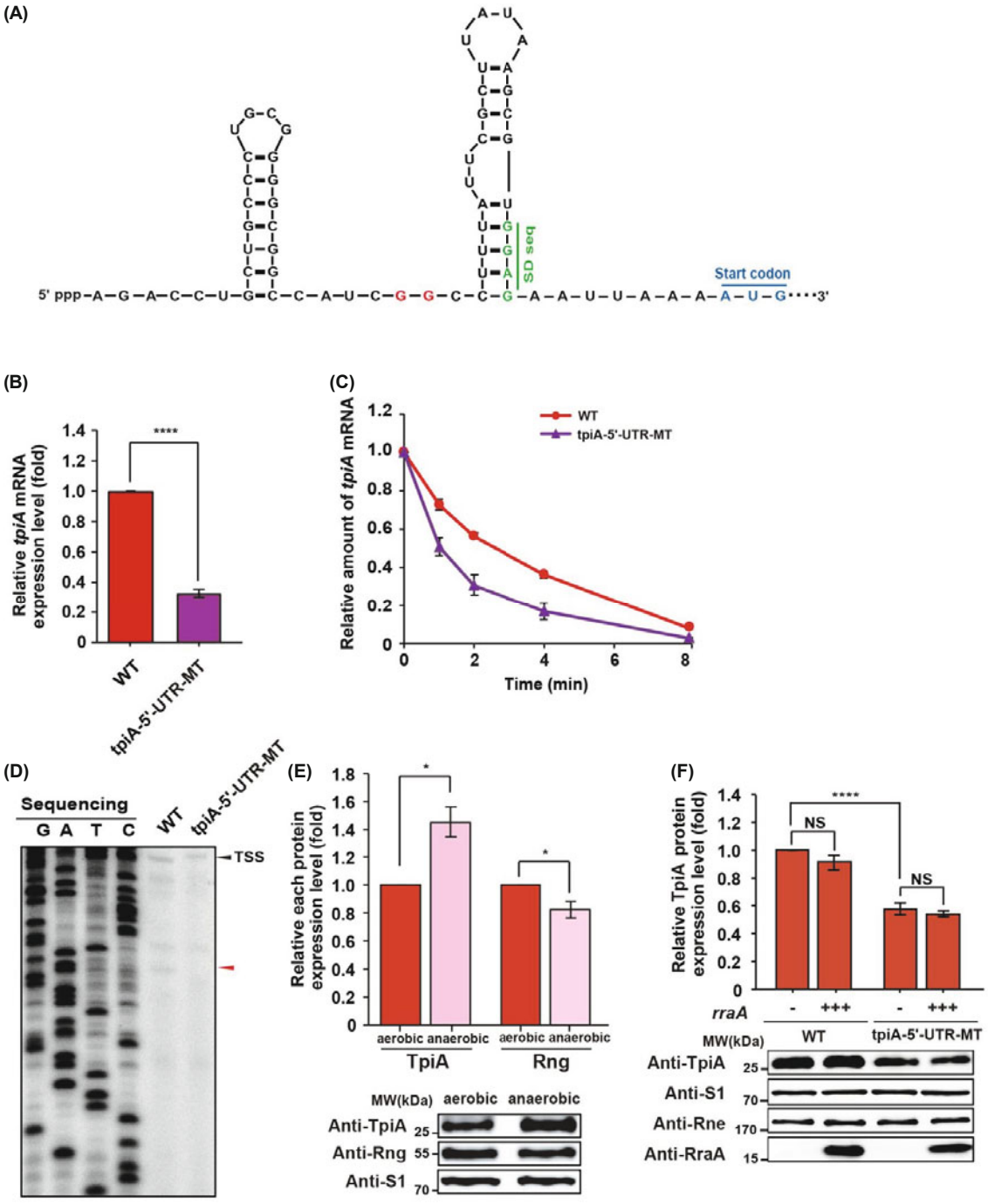

Fig. 3. Effects of a mutation in the 5′ UTR and oxygen availability on *tpiA* expression. (A) Alterations in the putative secondary structure of tpiA-5′-UTR-MT were predicted using M-fold software. Yellow-colored nucleotides indicate the location of the substituted nucleotides (UU to GG). (B) Analysis of *tpiA* mRNA expression levels. Total RNA was extracted from wild-type (WT) and tpiA-5′-UTR-MT-expressing cells cultured to an OD_{600} of 0.7. cDNA synthesis was performed and quantitated as described in the legend to Fig. 1A. (C) Comparison of *tpiA* mRNA stability between the WT and tpiA-5′-UTR-MT strains. Total RNA was prepared from *E. coli* cultures used in (B). cDNA synthesis was performed and quantitated as described in the legend to Fig. 1A. (D) Primer extension analysis of the 5′ UTR of tpiA-5′-UTR-MT *in vivo*. Primer extension analysis was performed as described in the legend to Fig. 2A. Black and red arrows indicate the TSS of *tpiA* mRNA and the RNase G cleavage product, respectively. (E) TpiA and Rng protein expression profiles under aerobic and anaerobic conditions. WT cells were cultured to mid-log phase under aerobic (OD_{600} = 2.0) and anaerobic conditions (OD_{600} = 0.4), and western blotting was performed using the respective polyclonal antibodies. The TpiA and Rng levels were compared by setting those of the WT strain grown under aerobic condition to 1. (F) Western blot analysis of TpiA in WT and tpiA-5′-UTR-MT cells with RraA overexpression. WT and tpiA-5′-UTR-MT strains harboring an empty vector (pKAN6B) or pKAN6-rraA were cultured to early log phase; L-arabinose (10 mM final concentration) was then added to induce the expression of the RraA protein, followed by incubation to an OD_{600} of 0.7. The cells were then collected for TpiA, Rne, and RraA western blot analysis using the respective polyclonal antibodies. The levels of TpiA, Rne, and RraA were compared by setting that of WT cells harboring pKAN6B to 1. For (E) and (F), S1 protein was used as an internal standard. For (B), (C), (E), and (F), data represent the mean ± s. e. m. of three independent experiments. Asterisks indicate significant differences (two-sided, unpaired Student's *t*-test), $^{*}P < 0.05$, $^{****}P < 0.0001$.

IPTG and pCas was cured by incubating for 9 h at 37°C.

Quantification and statistical analyses

The statistical details for all the experiments are included in the figure legends. Multiple comparison analysis was performed using SAS v. 9.2 with the Student-Newman-Keuls test (SAS Institute), and the Student's *t*-test was used for comparisons with controls using SAS v. 9.2 and SigmaPlot 10.0 (Systat Software). The data are presented as the mean ± s. e. m. and $P < 0.05$ was considered to indicate significance as previously described (Ramasamy *et al.*, 2017; Yi *et al.*, 2017).

Results

Negative regulation of *tpiA* gene expression by RNase G

To examine whether RNase G affects *tpiA* expression, we quantified *tpiA* mRNA and protein steady-state levels in the WT and *rng*-deleted (Δ*rng*) strains by real-time RT-PCR and western blot, respectively. Consistent with a previous genome-wide analysis (Lee *et al.*, 2002), *tpiA* mRNA abundance in the Δ*rng* strain increased approximately 1.4-fold compared to that of the WT strain (Fig. 1A). The TpiA protein level also increased by an extent comparable to that of the mRNA abundance (Fig. 1B). Next, the *tpiA* mRNA half-life was measured to determine whether the increased steady-state mRNA levels are a consequence of increased mRNA stability. We quantified *tpiA* mRNA by harvesting total RNA at each time point after rifampicin addition. As shown in Fig. 1C, the *tpiA* mRNA half-life in the Δ*rng* strain increased by approximately threefold compared to that of the WT strain (7.5 min vs 2.5 min), indicating a good correlation between *tpiA* mRNA abundance and stability.

Identification of RNase G cleavage site on *tpiA* mRNA

Next, we explored the location of the *cis*-acting elements in *tpiA* mRNA that are recognized by RNase G. Because RNase G is known to preferentially cleave AU-rich sequences in the 5′ UTRs of substrate mRNAs (Ito *et al.*, 2013; Clarke *et al.*, 2014), we performed a primer extension analysis using a ^{32}P-5′-end-labeled primer (tpiA+21R) that binds downstream of the *tpiA* start codon. We observed one distinct cDNA band that was present only in the lane loaded with WT cell-derived cDNA (Fig. 2A, left panel). Furthermore, in the Δ*rng* strain, we also observed an approximately 40% increase in the intensity of cDNA bands corresponding to the transcriptional start site (TSS) of the *tpiA* gene (Fig. 2A, left panel), similar to that previously proposed (Mendoza-Vargas *et al.*, 2009; Song *et al.*, 2014). These results indicate that RNase G cleaves between two U residues in the 5′ UTR of *tpiA* mRNA (Fig. 2A, right panel). This RNase G cleavage site is located in a single-stranded region between two stem-loop structures in the secondary structure of full-length *tpiA* mRNA, as inferred using the M-fold program (http://unafold.rna.albany.edu) (Zuker, 2003).

To demonstrate biochemically the cleavage of *tpiA* mRNA by RNase G, an *in vitro* cleavage assay was performed using a synthetic model RNA of *tpiA* mRNA (Fig. 2B, right panel). This synthetic RNA has 52 nucleotides of the 5′ UTR of *tpiA* mRNA including two stem-loops and the RNase G cleavage site. It was designed to have a minimal sequence of the *tpiA* mRNA 5′ UTR, without interfering with RNase G activity, to facilitate mapping of the RNase G cleavage site. Putative stem-loop structures were included because the ribonucleolytic activity of RNase E-like enzymes is known to be affected by adjacent stem-loops present in the cleavage site (McDowall *et al.*, 1994). It was labeled with ^{32}P at the 5′ end and incubated with purified RNase G. The results showed that RNase G cleaved the synthetic RNA at the site corresponding to that identified by primer extension analysis of *tpiA* mRNA (Fig. 2B). When RNA fragments generated by ribonucleases A and T1 digestion of the synthetic RNA, we also observed that overall secondary structure of the *tpiA* mRNA 5′ UTR deduced using the M-fold program is comparable to that of the synthetic RNA (Fig. 2A and B, right panels). Collectively, these results show that RNase G cleaves at a site located in the 5′ UTR of *tpiA* mRNA.

Effects of nucleotide substitutions in the RNase G cleavage site on *tpiA* mRNA stability

Although RNase G is known to preferentially cleave AU-rich, single-stranded region, the RNA structural determinants for RNase G cleavage activity have not been characterized. Consequently, we tested RNase G cleavage activity on *tpiA* mRNA containing U to G substitutions in the cleavage site of *tpiA* mRNA, which potentially destabilizes the lower part of the first stem-loop structure in the 5′ UTR (Fig. 3A). When the CRISPR-Cas9-induced mutant *tpiA* mRNA was expressed from tpiA-5′-UTR-MT (Wang *et al.*, 2018), its steady-state levels decreased by approximately 70% compared to that of the WT *tpiA* mRNA (Fig. 3B). This decreased mutant *tpiA* mRNA abundance likely resulted from destabilization of the mRNA, as the half-life of the mutant *tpiA* mRNA was shortened to 1.0 min compared to that of the WT *tpiA* mRNA (2.5 min) (Fig. 3C). Primer extension analysis of the mutant *tpiA* mRNA revealed the loss of cDNA synthesized from the RNase G cleavage product, indicating that alterations in the secondary structure of the *tpiA* mRNA 5′ UTR resulted in the loss of RNase G cleavage activity in the 5′ UTR (Fig. 3D). The decreased stability of *tpiA* mRNA by introduction of nucleotide substitutions was unexpected; this result may stem from destabilization of the first-stem loop structure, facilitating *tpiA* mRNA degradation by other ribonuclease(s) (See Discussion).

Regulation of *tpiA* expression by oxygen availability

E. coli is known to be a facultative anaerobe, producing chemical energy *via* the activation of glycolysis and fermentation under anaerobic conditions. To achieve this, *E. coli* cells likely enhance the production of glycolytic enzymes, including TpiA, when grown anaerobically. Therefore, we tested whether oxygen availability affects the RNase G-mediated regulation of *tpiA* expression by measuring the steady-state levels of the RNase G and TpiA proteins in WT cells under both aerobic and anaerobic conditions. Western blot analysis showed that, compared to WT *E. coli* cells grown under aerobic conditions, TpiA expression increased by 40% in

those grown under anaerobic conditions, coincident with a 20% decrease in RNase G expression levels (Fig. 3E). These results suggest that *tpiA* was upregulated as a consequence of the decreased RNase G expression under anaerobic condition in *E. coli*.

Discussion

The negative regulation of *tpiA* expression by RNase G at the posttranscriptional level has been previously suggested in *E. coli* (Lee *et al.*, 2002). In this study, we unveiled the molecular mechanism underlying the RNase G-mediated posttranscriptional regulation of *tpiA* expression, whereby RNase G affects *tpiA* mRNA stability by cleaving its 5′ UTR. We additionally discovered that exposing *E. coli* cells to conditions of low oxygen results in the upregulation of *tpiA* expression, which coincides with decreased levels of RNase G protein. The fact that enolase mRNA and protein abundance are negatively regulated by RNase G (Kaga *et al.*, 2002; Lee *et al.*, 2002), together with the results of the current study, indicates that RNase G plays an important role in facilitating glycolysis under anaerobic conditions by stabilizing mRNAs encoding glycolytic enzymes.

Nucleotide substitutions in the RNase G cleavage site that altered the secondary structure of the 5′ UTR resulted in decreased *tpiA* mRNA stability (Fig. 3A–C). This decreased stability of *tpiA* mRNA through the prevention of RNase G cleavage activity may stem from the destabilization of the first stem-loop structure by nucleotide substitutions, which leads to a *tpiA* mRNA structure vulnerable to degradation by other ribonucleases. One such a ribonuclease is RNase E, the activity of which is inhibited by adjacent stem-loops present in the RNase E cleavage site (McDowall *et al.*, 1994). RNase E is also known to be associated with expression of glycolytic enzymes: RNase E decays *ptsG* mRNA, which encodes the major glucose transporter, when the glycolytic pathway is blocked and RNase E-deficient cells show reduced phosphoenolpyruvate carboxylase production (Morita *et al.*, 2004; Tamura *et al.*, 2013). However, we observed that TpiA expression was not significantly changed when RraA, a protein inhibitor of RNase E (Lee *et al.*, 2003; Gorna *et al.*, 2010; Seo *et al.*, 2017; Park *et al.*, 2017; Song *et al.*, 2017), was overexpressed in the tpiA-5′-UTR-MT strain (Fig. 3F), indicating that alterations in the secondary structure of the 5′ UTR did not affect RNase E ribonucleolytic activity on *tpiA* mRNA. Inhibition of RNase E activity by RraA overexpression did not affect TpiA expression, either (Fig. 3F). These results indicate that that multiple layers of the mRNA quality control exist for expression of this key glycolytic enzyme and a few nucleotide substitutions in mRNA can dramatically alter mRNA degradation pathways. Further studies are needed to unveil the detailed mechanisms underlying this RNases-mediated regulatory pathway for *tpiA* expression.

Acknowledgements

We thank Drs. Minho Lee and Ji-Hyun Yeom for technical assistance. This research was supported by the National Research Foundation of Korea (NRF-2018R1A5A1025077). This research was also supported by the Chung-Ang University research grant in 2017.

References

Baek, J., Choi, E., and Lee, E.J. 2018. A rule governing the FtsH-mediated proteolysis of the MgtC virulence protein from *Salmonella enterica* serovar Typhimurium. *J. Microbiol.* **56**, 565–570.

Bernstein, J.A., Khodursky, A.B., Lin, P.H., Lin-Chao, S., and Cohen, S.N. 2002. Global analysis of mRNA decay and abundance in *Escherichia coli* at single-gene resolution using two-color fluorescent DNA microarrays. *Proc. Natl. Acad. Sci. USA* **99**, 9697–9702.

Cha, J.S., Pujol, C., and Kado, C.I. 1997. Identification and characterization of a *Pantoea citrea* gene encoding glucose dehydrogenase that is essential for causing pink disease of pineapple. *Appl. Environ. Microbiol.* **63**, 71–76.

Cho, M., Hu, G., Caza, M., Horianopoulos, L.C., Kronstad, J.W., and Jung, W.H. 2018. Vacuolar zinc transporter Zrc1 is required for detoxification of excess intracellular zinc in the human fungal pathogen *Cryptococcus neoformans*. *J. Microbiol.* **56**, 65–71.

Clarke, J.E., Kime, L., Romero, A.D., and McDowall, K.J. 2014. Direct entry by RNase E is a major pathway for the degradation and processing of RNA in *Escherichia coli*. *Nucleic Acids Res.* **42**, 11733–11751.

Deutscher, M.P. 2006. Degradation of RNA in bacteria: comparison of mRNA and stable RNA. *Nucleic Acids Res.* **34**, 659–666.

Gorna, M.W., Pietras, Z., Tsai, Y.C., Callaghan, A.J., Hernandez, H., Robinson, C.V., and Luisi, B.F. 2010. The regulatory protein RraA modulates RNA-binding and helicase activities of the *E. coli* RNA degradosome. *RNA* **16**, 553–562.

Hui, M.P., Foley, P.L., and Belasco, J.G. 2014. Messenger RNA degradation in bacterial cells. *Annu. Rev. Genet.* **48**, 537–559.

Ito, K., Hamasaki, K., Kayamori, A., Nguyen, P.A., Amagai, K., and Wachi, M. 2013. A secondary structure in the 5′ untranslated region of *adhE* mRNA required for RNase G-dependent regulation. *Biosci. Biotechnol. Biochem.* **77**, 2473–2479.

Jain, C. 2002. Degradation of mRNA in *Escherichia coli*. *IUBMB Life* **54**, 315–321.

Jiang, Y., Chen, B., Duan, C., Sun, B., Yang, J., and Yang, S. 2015. Multigene editing in the *Escherichia coli* genome via the CRISPR-Cas9 system. *Appl. Environ. Microbiol.* **81**, 2506–2514.

Kaga, N., Umitsuki, G., Nagai, K., and Wachi, M. 2002. RNase G-dependent degradation of the eno mRNA encoding a glycolysis enzyme enolase in *Escherichia coli*. *Biosci. Biotechnol. Biochem.* **66**, 2216–2220.

Kushner, S.R. 2004. mRNA decay in prokaryotes and eukaryotes: different approaches to a similar problem. *IUBMB Life* **56**, 585–594.

Lee, K., Bernstein, J.A., and Cohen, S.N. 2002. RNase G complementation of *rne* null mutation identifies functional interrelationships with RNase E in *Escherichia coli*. *Mol. Microbiol.* **43**, 1445–1456.

Lee, K., Zhan, X., Gao, J., Qiu, J., Feng, Y., Meganathan, R., Cohen, S.N., and Georgiou, G. 2003. RraA. a protein inhibitor of RNase E activity that globally modulates RNA abundance in *E. coli*. *Cell* **114**, 623–634.

Li, Z., Pandit, S., and Deutscher, M.P. 1999. RNase G (CafA protein) and RNase E are both required for the 5′ maturation of 16S ribosomal RNA. *EMBO J.* **18**, 2878–2885.

Lim, B., Sim, M., Lee, H., Hyun, S., Lee, Y., Hahn, Y., Shin, E., and Lee, K. 2015. Regulation of *Escherichia coli* RNase III activity. *J. Microbiol.* **53**, 487–494.

McDowall, K.J., Kaberdin, V.R., Wu, S.W., Cohen, S.N., and Lin-Chao, S. 1995. Site-specific RNase E cleavage of oligonucleotides and inhibition by stem-loops. *Nature* **374**, 287–290.

McDowall, K.J., Lin-Chao, S., and Cohen, S.N. 1994. A+U content rather than a particular nucleotide order determines the specificity of RNase E cleavage. *J. Biol. Chem.* **269**, 10790–10796.

Mendoza-Vargas, A., Olvera, L., Olvera, M., Grande, R., Vega-Alvarado, L., Taboada, B., Jimenez-Jacinto, V., Salgado, H., Juarez, K., Contreras-Moreira, B., *et al.* 2009. Genome-wide identification of transcription start sites, promoters and transcription factor binding sites in *E. coli*. *PLoS One* **4**, e7526.

Mohanty, B.K. and Kushner, S.R. 2016. Regulation of mRNA decay in bacteria. *Annu. Rev. Microbiol.* **70**, 25–44.

Morita, T., Kawamoto, H., Mizota, T., Inada, T., and Aiba, H. 2004. Enolase in the RNA degradosome plays a crucial role in the rapid decay of glucose transporter mRNA in the response to phosphosugar stress in *Escherichia coli*. *Mol. Microbiol.* **54**, 1063–1075.

Park, N., Heo, J., Song, S., Jo, I., Lee, K., and Ha, N.C. 2017. Crystal structure of *Streptomyces coelicolor* RraAS2, an unusual member of the RNase E inhibitor RraA protein family. *J. Microbiol.* **55**, 388–395.

Ramasamy, S., Arumugam, A., and Chandran, P. 2017. Optimization of *Enterobacter cloacae* (KU923381) for diesel oil degradation using response surface methodology (RSM). *J. Microbiol.* **55**, 104–111.

Seo, S., Kim, D., Song, W., Heo, J., Joo, M., Lim, Y., Yeom, J.H., and Lee, K. 2017. RraAS1 inhibits the ribonucleolytic activity of RNase ES by interacting with its catalytic domain in *Streptomyces coelicolor*. *J. Microbiol.* **55**, 37–43.

Sharan, S.K., Thomason, L.C., Kuznetsov, S.G., and Court, D.L. 2009. Recombineering: a homologous recombination-based method of genetic engineering. *Nat. Protoc.* **4**, 206–223.

Sim, S.H., Yeom, J.H., Shin, C., Song, W.S., Shin, E., Kim, H.M., Cha, C.J., Han, S.H., Ha, N.C., Kim, S.W., *et al.* 2010. *Escherichia coli* ribonuclease III activity is downregulated by osmotic stress: consequences for the degradation of *bdm* mRNA in biofilm formation. *Mol. Microbiol.* **75**, 413–425.

Song, S., Hong, S., Jang, J., Yeom, J.H., Park, N., Lee, J., Lim, Y., Jeon, J.Y., Choi, H.K., Lee, M., *et al.* 2017. Functional implications of hexameric assembly of RraA proteins from *Vibrio vulnificus*. *PLoS One* **12**, e0190064.

Song, W., Joo, M., Yeom, J.H., Shin, E., Lee, M., Choi, H.K., Hwang, J., Kim, Y.I., Seo, R., Lee, J.E., *et al.* 2019. Divergent rRNAs as regulators of gene expression at the ribosome level. *Nat. Microbiol.* **4**, 515–526.

Song, W., Kim, Y.H., Sim, S.H., Hwang, S., Lee, J.H., Lee, Y., Bae, J., Hwang, J., and Lee, K. 2014. Antibiotic stress-induced modulation of the endoribonucleolytic activity of RNase III and RNase G confers resistance to aminoglycoside antibiotics in *Escherichia coli*. *Nucleic Acids Res.* **42**, 4669–4681.

Sun, J., Wang, W., Yao, C., Dai, F., Zhu, X., Liu, J., and Hao, J. 2018. Overexpression and characterization of a novel cold-adapted and salt-tolerant GH1 β-glucosidase from the marine bacterium *Alteromonas* sp. L82. *J. Microbiol.* **56**, 656–664.

Tamura, M., Moore, C.J., and Cohen, S.N. 2013. Nutrient dependence of RNase E essentiality in *Escherichia coli*. *J. Bacteriol.* **195**, 1133–1141.

Tock, M.R., Walsh, A.P., Carroll, G., and McDowall, K.J. 2000. The CafA protein required for the 5′-maturation of 16S rRNA is a 5′-end-dependent ribonuclease that has context-dependent broad sequence specificity. *J. Biol. Chem.* **275**, 8726–8732.

Wachi, M., Umitsuki, G., and Nagai, K. 1997. Functional relationship between *Escherichia coli* RNase E and the CafA protein. *Mol. Gen. Genet.* **253**, 515–519.

Wachi, M., Umitsuki, G., Shimizu, M., Takada, A., and Nagai, K. 1999. *Escherichia coli cafA* gene encodes a novel RNase, designated as RNase G, involved in processing of the 5′ end of 16S rRNA. *Biochem. Biophys. Res. Commun.* **259**, 483–488.

Wang, X., He, J., and Le, K. 2018. Making point mutations in *Escherichia coli* BL21 genome using the CRISPR-Cas9 system. *FEMS Microbiol. Lett.* **365**, fny060.

Yeom, J.H., Go, H., Shin, E., Kim, H.L., Han, S.H., Moore, C.J., Bae, J., and Lee, K. 2008. Inhibitory effects of RraA and RraB on RNAse E-related enzymes imply conserved functions in the regulated enzymatic cleavage of RNA. *FEMS Microbiol. Lett.* **285**, 10–15.

Yeom, J.H. and Lee, K. 2006. RraA rescues *Escherichia coli* cells over-producing RNase E from growth arrest by modulating the ribonucleolytic activity. *Biochem. Biophys. Res. Commun.* **345**, 1372–1376.

Yi, Y.J., Lim, J.M., Gu, S., Lee, W.K., Oh, E., Lee, S.M., and Oh, B.T. 2017. Potential use of lactic acid bacteria *Leuconostoc mesenteroides* as a probiotic for the removal of Pb(II) toxicity. *J. Microbiol.* **55**, 296–303.

Zuker, M. 2003. Mfold web server for nucleic acid folding and hybridization prediction. *Nucleic Acids Res.* **31**, 3406–3415.